HHS Public Access

Author manuscript

Cell Metab. Author manuscript; available in PMC 2018 April 04.

Published in final edited form as:

Cell Metab. 2017 April 04; 25(4): 935–944.e4. doi:10.1016/j.cmet.2017.03.005.

FGF21 Regulates Metabolism Through Adipose-Dependent and -Independent Mechanisms

Lucas D. BonDurant[1,2,5], **Magdalene Ameka**[1,2,5], **Meghan C. Naber**[1,2], **Kathleen R. Markan**[1,2], **Sharon O. Idiga**[1,2], **Michael R. Acevedo**[3], **Susan A. Walsh**[3], **David M. Ornitz**[4], and **Matthew J. Potthoff**[1,2,*]

[1]Department of Pharmacology, University of Iowa Carver College of Medicine, Iowa City, IA 52242, USA

[2]Fraternal Order of Eagles Diabetes Research Center, University of Iowa Carver College of Medicine, Iowa City, IA 52242, USA

[3]Department of Small Animal Imaging Core, University of Iowa Carver College of Medicine, Iowa City, IA 52242, USA

[4]Department of Developmental Biology, Washington University School of Medicine, St. Louis, MO 63110, USA

SUMMARY

FGF21 is an endocrine hormone that regulates energy homeostasis and insulin sensitivity. The mechanism of FGF21 action and the tissues responsible for these effects have been controversial, with both adipose tissues and the central nervous system being identified as the target site mediating FGF21-dependent increases in insulin sensitivity, energy expenditure, and weight loss. Here we show that while FGF21 signaling to adipose tissue is required for the acute insulin sensitizing effects of FGF21, FGF21 signaling to adipose tissue is not required for its chronic effects to increase energy expenditure and lower body weight. Also, in contrast to previous studies, we found that adiponectin is dispensable for the metabolic effects of FGF21 in increasing insulin sensitivity and energy expenditure. Instead, FGF21 acutely enhances insulin sensitivity through actions on brown adipose tissue. Our data reveal that the acute and chronic effects of FGF21 can be dissociated through adipose-dependent and -independent mechanisms.

eTOC Paragraph

[*]Lead Contact: Matthew J. Potthoff, University of Iowa Carver College of Medicine, 169 Newton Road, 3322 PBDB, Iowa City, IA 52242, Phone: 319-384-4438, Fax: 319-335-8930, matthew-potthoff@uiowa.edu.

[5]Co-first authors

AUTHOR CONTRIBUTIONS

L.D.B. and M.A. designed and performed experiments, interpreted data, and wrote the paper. M.C.N., K.R.M., S.O.I., M.R.A., and S.A.W. performed experiments and interpreted data. D.M.O contributed essential reagents. M.J.P. conceived of the project, designed and performed experiments, interpreted data, wrote the paper, and is responsible for the integrity of its content.

Pharmacological administration of FGF21 increases insulin sensitivity and promotes weight loss. BonDurant et al. show that FGF21 signaling to adipose tissues is essential for the acute insulin-sensitizing effects of FGF21, but not its effects on body weight. Importantly, loss of FGF21 signaling specifically to brown adipocytes disrupts FGF21-mediated glucose disposal.

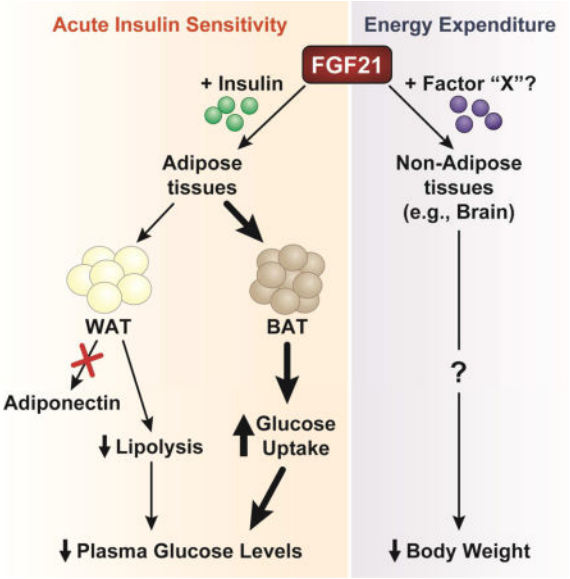

INTRODUCTION

The body possesses at least three distinct types of adipocytes: white, beige/brite, and brown adipocytes. White adipocytes function to store energy, while brown adipocytes dissipate energy as heat through a process known as adaptive thermogenesis (Rosen and Spiegelman, 2014). This is accomplished by inducing the expression of mitochondrial uncoupling protein 1 (UCP1), a protein which releases chemical energy as heat by destroying the mitochondrial inner membrane hydrogen gradient (Cannon and Nedergaard, 2004). Brown-like adipocytes, termed beige/brite adipocytes, appear in white adipose depots in response to various signals and also express UCP1. Brown adipose tissue (BAT) depots in rodents (Bartelt et al., 2011) and humans (Orava et al., 2011) increase glucose uptake when activated and are highly insulin sensitive. Insulin administration alone in humans is sufficient to stimulate glucose uptake in BAT comparable to the rate of glucose uptake in skeletal muscle (Orava et al., 2011). Thus, there is significant interest in identifying strategies to safely activate BAT to increase energy expenditure and fuel utilization.

FGF21 is an important regulator of energy homeostasis and a potential therapeutic target for the treatment of metabolic disease. Multiple studies have demonstrated that pharmacological administration of FGF21 to obese and diabetic animal models markedly improves carbohydrate and lipid homeostasis and promotes weight loss (reviewed in (Markan and Potthoff, 2015)). Interestingly, FGF21 has both acute and chronic effects on metabolism. Administration of a single pharmacological dose of FGF21 to obese mice is sufficient to rapidly improve insulin sensitivity and decrease plasma glucose levels by over 50 percent (Xu et al., 2009b). In contrast to its acute effects, chronic administration of FGF21 in animal

models increases energy expenditure and causes weight loss (Coskun et al., 2008; Xu et al., 2009a), and therefore secondarily increases insulin sensitivity. FGF21-based mimetics have also been shown to improve metabolic profiles and decrease body weight in humans, demonstrating the therapeutic relevance of FGF21 target pathways (Gaich et al., 2013; Talukdar et al., 2016). FGF21 functions by signaling through a receptor complex composed of fibroblast growth factor receptor 1 (FGFR1) and the co-receptor β-klotho, both of which are required for FGF21 signaling (Kurosu et al., 2007; Ogawa et al., 2007). Activation of this receptor complex initiates a signaling cascade resulting in the phosphorylation of FGF receptor substrate 2α and ERK1/2. However, the target tissues mediating the effects of FGF21 are unclear.

Currently, both adipose tissues and the central nervous system (CNS) have been proposed to be important sites of action for the metabolic effects of FGF21. However, the studies examining the importance of FGF21 signaling to adipose tissues were confounded by the use of ap2-Cre mice (Adams et al., 2012b; Ding et al., 2012) which drive Cre expression in non-adipose tissues, including the CNS (Harno et al., 2013). Consistent with adipose tissue being an important FGF21 target, the adipokine adiponectin was shown to be required for the effects of FGF21 on improving glucose homeostasis and insulin sensitivity following either acute or chronic FGF21 administration (Holland et al., 2013; Lin et al., 2013). Using mice that lack the obligate FGF21 co-receptor, β-klotho, specifically in adipose tissues, we show that FGF21 requires direct signaling to adipose tissues for its acute insulin-sensitizing effects. However, in contrast to previous reports, we show that plasma adiponectin levels are not increased in response to acute FGF21 administration and that both the acute and chronic metabolic effects of FGF21 are mediated independent of adiponectin. Importantly, while FGF21 signaling to adipose tissue is required for its acute insulin-sensitizing effects, FGF21-mediated increases in energy expenditure and secondary improvements in insulin sensitivity are adipose-independent. These data provide important insights into the mechanism of FGF21 action and identify the contribution of adipose tissues to the metabolic effects of FGF21.

RESULTS

The acute insulin sensitizing effects of FGF21 require direct signaling to adipose tissues

To determine the metabolic effects of direct FGF21 signaling to adipose tissue, we generated mice lacking the obligate FGF21 co-receptor, β-klotho (gene symbol: *Klb*), specifically in adipose tissue (KLB AdipoKO mice) by crossing $KLB^{fl/fl}$ mice with Adiponectin-Cre transgenic mice. As expected, *β-klotho* mRNA (Fig. 1A) and protein levels (Fig. S1A) were ablated specifically in adipose tissue depots of KLB AdipoKO mice. In addition, FGF21-mediated phosphorylation of ERK1/2 in white adipose tissue (WAT; Fig. 1B) and induction of known downstream early response genes (i.e., *Egr1* and *cFos*) were abolished specifically in adipose tissues of KLB AdipoKO mice (Fig. S1B–D). Lean wild-type (WT) and KLB AdipoKO mice showed no significant differences in body weight (Fig. S1E) or basal insulin sensitivity (Fig. S1F). To determine whether FGF21 signaling directly to adipose tissue is required for the acute insulin sensitizing effects of FGF21, we co-administered FGF21 and insulin to WT and KLB AdipoKO mice. Acute administration of FGF21 enhanced insulin

sensitivity in WT mice, and this effect was markedly impaired in lean KLB AdipoKO mice (Fig. 1C). Diet-induced obese (DIO) WT and KLB AdipoKO mice also did not have significant differences in body weight (Fig. S1G), or basal insulin sensitivity (Fig. S1H). However, acute administration of FGF21 to DIO WT mice markedly enhanced insulin sensitivity whereas this effect was ablated in DIO KLB AdipoKO mice (Fig. 1D). Thus, FGF21 signaling to adipose tissue is required for the acute insulin sensitizing effects of FGF21.

Adiponectin is not required for the metabolic effects of FGF21

Circulating adiponectin levels were reported to increase in response to acute administration of FGF21 (Holland et al., 2013; Lin et al., 2013). To confirm this observation, we examined adiponectin levels in lean and DIO WT mice in response to a single injection of recombinant FGF21. In contrast to previous reports, we found that acute administration of FGF21 had no significant effect on plasma adiponectin levels in either lean or DIO WT mice (Fig. 1E,F). In addition, treatment of primary white adipocytes with FGF21 did not significantly increase levels of adiponectin in the media (Fig. S1I). We next examined whether adiponectin was required for the acute insulin sensitizing effects of FGF21 by administering FGF21 to mice lacking adiponectin. Administration of FGF21 to Adiponectin knockout (Adipoq KO) mice resulted in the same increase in insulin sensitivity as observed in WT mice (Fig. 1G and S1J). Thus, our data demonstrates that adiponectin is not required for the acute insulin sensitizing effects of FGF21.

To determine whether adiponectin is required for the chronic effects of FGF21 in increasing energy expenditure and improving insulin sensitivity, we administered FGF21 to DIO WT and Adipoq KO mice for three weeks by daily intraperitoneal (i.p.) injection. FGF21 administration did not induce plasma adiponectin (Fig. 2A) or *Adipoq* mRNA levels in WT mice (Fig. 2B), and as expected, circulating adiponectin levels (Fig. 2A) and *Adipoq* mRNA levels (Fig. 2B) were completely abolished in Adipoq KO mice. Consistent with previous reports, administration of FGF21 to DIO WT mice resulted in significant weight loss, and this effect of FGF21 was recapitulated in DIO Adipoq KO mice (Fig. 2C,D). In addition, FGF21 administration reduced fat mass (Fig. 2E), lowered hepatic triglyceride levels (Fig. 2F), lowered plasma cholesterol levels (Fig. 2G), and reduced plasma insulin and leptin levels (Fig. 2H,I) in both DIO WT and Adipoq KO mice. FGF21 target genes that regulate BAT metabolism, including *bone morphogenic protein 8b (Bmp8b)* and *zinc finger and BTB domain containing 16 (Zbtb16)* (Muise et al., 2013), were also induced in both DIO WT and Adipoq KO mice (Fig. S2). In contrast to previous reports (Holland et al., 2013; Lin et al., 2013), insulin tolerance tests in these groups of mice revealed that FGF21 also effectively improved insulin sensitivity in both DIO WT and Adipoq KO mice (Fig. 2J). Therefore, adiponectin is not required for the chronic effects of FGF21 to reduce body weight or its effects on glucose homeostasis and insulin sensitivity.

Direct FGF21 signaling to adipose tissue is not required to promote weight loss and improve metabolic profiles—Since FGF21 signaling to adipose tissue is required for its acute insulin sensitizing effects, we next assessed whether direct signaling to adipose tissue is also required for the beneficial effects of chronic FGF21 treatment. FGF21

was administered continuously to DIO WT and KLB AdipoKO mice by osmotic minipumps for 2 weeks. Delivery of FGF21 resulted in comparable levels of circulating FGF21 in both DIO WT and KLB AdipoKO mice (Fig. 3A). In contrast to daily administration of FGF21 via i.p. injection (Fig. 2A), continuous administration of FGF21 via osmotic minipumps resulted in a significant increase in plasma adiponectin levels in DIO WT mice (Fig. 3B). However, this increase in plasma adiponectin in response to continuous FGF21 administration was absent in DIO KLB AdipoKO mice (Fig. 3B). Despite the lack of induction of plasma adiponectin levels, continuous administration of FGF21 to DIO KLB AdipoKO mice still markedly lowered body weight (Fig. 3C), decreased hepatic (Fig. 3D) and plasma triglycerides (Fig. 3E), and lowered plasma glucose and insulin levels (Fig. 3F,G) compared to vehicle treated DIO KLB AdipoKO mice. Moreover, the magnitude of the metabolic improvements from FGF21 treatment was similar to that of DIO WT mice administered FGF21 (Fig. 3C–G). Plasma leptin levels were comparable in both DIO WT and KLB AdipoKO mice administered FGF21, although basal leptin levels were lower in DIO KLB AdipoKO mice (Fig. 3H). FGF21 administration also improved glucose tolerance (Fig. 3I,J and S3A,B) and insulin sensitivity (Fig. 3K,L) in response to extended FGF21 administration in both DIO WT and KLB AdipoKO mice. Together, these results demonstrate that extended, pharmacological administration of FGF21 does not require direct signaling to adipose tissue to stimulate weight loss and improve insulin sensitivity and glucose homeostasis in DIO mice. In addition, these data demonstrate that the potent triglyceride lowering effects of FGF21 through accelerated lipoprotein catabolism in white and brown adipose tissues (Schlein et al., 2016) is not mediated by direct signaling to adipose tissues.

FGF21 functions by preferentially signaling through a receptor complex composed of FGFR1 and β-klotho. Alternative strategies have been employed to activate FGFR1 directly through the use of activating antibodies as a potential therapeutic for diabetes and obesity (Wu et al., 2011). As adipose tissue has been reported to be an important site of action for these therapeutic modalities (Wu et al., 2011), we next employed an independent strategy to assess the importance of FGFR1-dependent signaling directly in adipose tissue. This was accomplished by generating transgenic mice that provide inducible, adipose-specific expression of a constitutively-active FGFR1 protein. Transgenic mice with a tetracycline operon driving a myc-tagged constitutively-active FGFR1 protein (TRE-caFGFR1) (Cilvik et al., 2013) were crossed with mice expressing rtTA specifically in adipose tissue using the adiponectin promoter (Adipo-rtTA) (Sun et al., 2012). The TRE-caFGFR1 transgenic mouse line produces a chimeric protein in which a ligand-independent, constitutively-active FGFR1 can be specifically induced through doxycycline (DOX) administration in rtTA-expressing cells (e.g., Adipo-rtTA/TRE-caFGFR1 double transgenic mice). Adipo-rtTA/TRE-caFGFR1 double transgenic mice express ca*FGFR1* mRNA transcript specifically in adipose tissues only in the presence of DOX (Fig. 3M). WT, TRE-caFGFR1 transgenic (TG), and Adipo-rtTA/TRE-caFGFR1 double TG mice were next induced to obesity by high fat diet (HFD) feeding in the absence of DOX. No significant differences in body weight (Fig. S3C) or composition (Fig. S3D) was observed between groups of mice. Subsequent administration of HFD containing DOX (HFD + DOX) for 2 weeks to DIO WT, TRE-caFGFR1 TG, and Adipo-rtTA/TRE-caFGFR1 double TG mice produced ca*FGFR1* mRNA transcript (Fig.

S3E) and protein levels (Fig. 3N and S3F) specifically in adipose tissues of Adipo-rtTA/TRE-caFGFR1 double TG mice. Expression of caFGFR1 protein in adipose tissue resulted in increased ERK1/2 phosphorylation (Fig. 3N) and early-response gene expression (Fig. 3O) similar to FGF21 administration (Fig. S1B). However, constitutive activation of FGFR1 signaling directly to adipose tissue produced no significant differences in body weight (Fig. 3P), hepatic (Fig. 3Q) or plasma triglycerides (Fig. S3G), insulin, or glucose levels (Fig. 3R,S) between DIO Adipo-rtTA/TRE-caFGFR1 double TG mice and control mice. Therefore, these data demonstrate that constitutive activation of FGFR1 signaling specifically in adipose tissues fails to induce the metabolic effects observed with chronic, pharmacological FGF21 administration.

FGF21 signals directly to brown adipocytes to acutely increase insulin sensitivity

Since adipose tissue is required for the acute, insulin sensitizing effects of FGF21, we next explored whether this effect was mediated through brown or white adipocytes. In contrast to Adiponectin-Cre transgenic mice which drive Cre expression in both white and brown adipocytes, UCP1-Cre transgenic mice express Cre recombinase in brown (and beige/brite) adipocytes. We therefore generated mice which lack β-klotho specifically in brown ($UCP1^{+}$) adipocytes (KLB BatKO) by crossing UCP1-Cre transgenic mice with $KLB^{fl/fl}$ mice. Importantly, *β-klotho* mRNA and protein levels, and early response gene expression in response to FGF21, were markedly reduced in BAT of KLB BatKO mice, whereas epididymal WAT *β-klotho* levels were unchanged in these same mice relative to littermate controls (Figs. 4A and S4A–D). Subcutaneous WAT exhibited an approximate 50% decrease in *β-klotho* mRNA expression (Fig. 4A). Consistent with KLB AdipoKO mice, lean WT and KLB BatKO mice showed no significant differences in basal insulin sensitivity (Fig. S4E). However, as observed with mice lacking KLB from all adipose tissues (KLB AdipoKO), co-administration of FGF21 with insulin failed to enhance insulin sensitivity in KLB BatKO mice (Fig. 4B and S4E). Thus, FGF21 signaling to brown adipocytes is required for the acute insulin sensitizing effects of FGF21.

We next used mice with adipose-specific deletion of the insulin receptor to examine whether insulin sensitization in adipose tissue accounts for the acute insulin sensitizing effects of FGF21. Adipose-specific insulin receptor knockout (IR AdipoKO) mice were generated by crossing $IR^{fl/fl}$ mice with Adiponectin-Cre mice (Fig. S4F). Notably, although IR AdipoKO mice exhibit basal hyperglycemia, they were completely refractory to the insulin sensitizing actions of FGF21 (Fig. 4C and S4G). These data demonstrate that functional insulin signaling in adipose tissue is required for the whole-body insulin sensitizing effects of FGF21.

To determine the site of glucose disposal in response to acute FGF21 administration, we performed PET/CT studies with [^{18}F]-FDG in WT and KLB BatKO mice following administration of vehicle or FGF21 in combination with insulin. Administration of FGF21 with insulin significantly increased BAT glucose uptake in WT mice compared to insulin plus vehicle, and this effect was abolished in KLB BatKO mice (Fig. 4D,E). We also independently assessed in vivo tissue-specific glucose uptake in WT and KLB BatKO mice by performing radioactive glucose uptake assays. Consistent with the PET/CT data, in vivo

radioactive glucose uptake in BAT was significantly increased in WT mice in response to co-administration of insulin plus FGF21, and this effect was abrogated in KLB BatKO (Fig. 4F). We did not observe increased glucose uptake in other adipose tissue depots and non-adipose tissues, except for the heart (Fig. 4F). These data demonstrate that FGF21 functions acutely to promote glucose uptake in BAT.

In summary, our results demonstrate that the acute and chronic metabolic effects of FGF21 can be dissociated through adipose-dependent and independent mechanisms. In contrast to previous studies (Adams et al., 2012b; Wu et al., 2011), we show that FGF21 signaling to adipose tissue is not required, and activation of FGFR1 signaling specifically in adipose tissue is not sufficient, to decrease body weight and induce the secondary improvements in insulin sensitivity and glucose homeostasis. Our data are therefore compatible with a report that FGF21 signaling to the CNS is important for its energy expending effects (Owen et al., 2014). While adipose tissues may not be directly targeted by FGF21 to increase energy expenditure, studies with lipodystrophic mice still suggest that adipose tissue is important for the metabolic effects of FGF21 (Veniant et al., 2012). These effects could be mediated through increases in adipose tissue metabolism (i.e., centrally activated adipose-tissue thermogenesis) or through the production of adipokines like leptin which may be important for the energy expending effects of FGF21 (Adams et al., 2012a). Thus, additional work is necessary to determine how FGF21 signals in the CNS to increase energy expenditure and how adipose tissues may contribute to these effects.

These studies also provide important insights into the acute insulin sensitizing effects of FGF21, revealing that adiponectin is not required for the effects of FGF21 on insulin sensitivity. Instead, our studies identify direct FGF21 signaling to UCP1+ adipocytes as being critical to enhance insulin sensitivity through insulin receptor signaling. The explanation for observed differences in adiponectin in this study and previous studies (Holland et al., 2013; Lin et al., 2013) is not immediately clear, but may reflect differences in dosing and/or source of recombinant FGF21, or use of different Adipoq KO mouse lines. Nevertheless, while adiponectin levels failed to increase in KLB AdipoKO mice in response to chronic administration of FGF21 by minipump (Fig. 3B), improvements in insulin sensitivity and glucose homeostasis were still observed (Fig. 3F,G and Fig. 3I,K). Conversely, in humans with obesity, administration of an FGF21 analog markedly increases plasma adiponectin levels without significantly changing plasma glucose levels (Talukdar et al., 2016). Instead, our finding that the acute, insulin sensitizing effects of FGF21 function through direct actions on brown/beige adipocytes may explain why administration of FGF21 analogues to humans, which possess relatively less BAT mass, results in less pronounced glucose-lowering effects compared to rodents (Gaich et al., 2013; Talukdar et al., 2016).

STAR METHODS

Contact for Reagent and Resource Sharing

Further information and requests for resources and reagents should be directed to and will be fulfilled by the Lead Contact, Matthew Potthoff (matthew-potthoff@uiowa.edu).

Experimental Model and Subject Details

All experiments presented in this study were conducted according to the animal research guidelines from NIH and were approved by the University of Iowa IACUC.

A total of 314 adult male mice and 14 four-day old pups (male and female) were used. Strain details and number of animals in each group are as follows:

40 Adiponectin KO mice (B6;129-*Adipoq*^{tm1Chan}/J)(Jackson laboratories stock #008195) (21 AdipoQ KO and 19 littermate controls (+/+ and +/−))

126 KLB AdipoKO mice (KLB$^{fl/fl;Adiponectin\text{-}Cre}$) (64 KLB$^{fl/fl;Adiponectin\text{-}Cre}$ and 62 KLB$^{fl/fl}$ littermate controls)

52 Adipo-FGFR1ca transgenic mice (Adipo-rtTA/TRE-caFGFR1 double transgenic mice) (19 Adipo-rtTA/TRE-caFGFR1 double transgenic mice and 33 littermate controls)

12 IR AdipoKO (IR$^{fl/fl;Adiponectin\text{-}Cre}$) (7 IR$^{fl/fl;Adiponectin\text{-}Cre}$ and 5 IR$^{fl/fl}$)

84 KLB BatKO (KLB$^{fl/fl;Ucp1\text{-}Cre}$) (39 KLB$^{fl/fl;Ucp1\text{-}Cre}$ and 45 KLB$^{fl/fl}$)

14 C57BL/6J pups

All mice used in experiments were individually housed under a 12 hr light/dark cycle. At the time of the experiments, animals were 11–21 weeks old, except for C57BL/6J pups, which were four days old. Littermates of the same sex were randomly assigned to experimental groups. Animal weights are reported in figures and supplemental figures. All animals were used in scientific experiments for the first time. This includes no previous exposures to pharmacological substances. High fat diets were provided to the indicated mice to induce mice to obesity. Health status was normal for all animals.

Method Details

Mouse Studies—Adiponectin KO (Ma et al., 2002), KLB$^{fl/fl}$ (Ding et al., 2012), Adiponectin-Cre (Eguchi et al., 2011), Adiponectin-rtTA (Sun et al., 2012), IR$^{fl/fl}$ (Bruning et al., 1998) and TRE-caFGFR1 mice (Cilvik et al., 2013) have been previously reported and were maintained on a C57Bl/6 genetic background. UCP1-Cre mice (stock #024670) were obtained from Jackson laboratory. Mice were either fed chow (Teklad 2920X) or a high-fat diet (HFD) consisting of 60% kcal from fat (Research Diets D12492) for 12 weeks to induce mice to obesity. For studies with Adiponectin-rtTA and TRE-caFGFR1 transgenic mice, groups of mice were fed a custom diet of 60% kcal from fat with 200 mg doxycycline (DOX)/kg (Research Diets) or given drinking water comprised of 10% sucrose and 0.2 mg/mL of DOX as indicated. Body composition was measured using a rodent-sized NMR machine (Bruker Minispec LF50). Male mice were used for all experiments. The ages of all mice used in the studies are as indicated in figure legends.

Administration of Recombinant Human FGF21—Recombinant FGF21 protein was generated and provided by Novo Nordisk. 16–18 week old WT and KLB AdipoKO male mice on HFD for 12 weeks were randomized by body weight to receive FGF21 via minipump. Mice were individually housed for one week before surgery and body

composition assessed via NMR. DIO mice were then subcutaneously implanted with osmotic minipumps (Alzet), containing recombinant human FGF21 (1mg/kg/day) or vehicle. All mice were then maintained in single housing with continued HFD feeding for two weeks. Body weights were recorded daily and body composition was assessed at the end of the two weeks.

For chronic i.p. administration of FGF21, 16–18 week old DIO WT and KLB AdipoKO mice and 16–18 week old DIO WT and Adiponectin KO mice on HFD for 12 weeks, were randomized by body weight to receive FGF21 or vehicle. Prior to the first injection, mice were individually caged for 5 days and body composition was assessed by NMR the day before the first treatment. All mice received either a single injection of FGF21 (1 mg/kg) or vehicle daily (09:00) for three weeks. Body weights were recorded daily and glucose and insulin tolerance tests performed at the times indicated in the figure legends. At the end of the three weeks, body composition was again assessed by NMR.

Insulin and Glucose Tolerance Tests—For co-injection studies of insulin and FGF21, mice were individually caged for 5 days prior to insulin plus vehicle co-injection in the indicated mice. On the day of the study, mice were fasted for 5 hours and time 0 blood collected via tail bleed. All mice were then i.p. injected with insulin (0.75U/kg BW for DIO mice and 0.25U/kg BW for lean mice) plus vehicle. Tail blood was collected at 15, 30, 60, 90, and 120 minutes post-injection. One week later, the same experimental paradigm was followed using the same cohorts of mice except all mice were administered insulin plus FGF21 (1 mg/kg). The same dose of insulin (0.75U/kg BW for DIO mice and 0.25U/kg BW for lean mice) was used for both the vehicle and FGF21 co-injections. Mice were maintained on the same diets throughout experiments. Same groups of mice were used in order to assess basal versus FGF21-stimulated insulin sensitivity. Plasma glucose was subsequently measured with a colorimetric assay (Wako).

For glucose and insulin tolerance tests in DIO mice, mice were fasted for 5 hours and then injected i.p. with 1.3g glucose/kg BW or 0.75U insulin/kg BW, respectively, and tail blood was collected at 0, 15, 30, 60, 90, and 120 minutes. Plasma glucose and insulin levels were subsequently measured with a colorimetric assay (Wako) and an Ultrasensitive Mouse Insulin ELISA (Crystal Chem Inc.), respectively.

Gene Expression—Gene expression analyses were performed as described (von Holstein-Rathlou et al., 2016). RNA was isolated from the indicated tissues following Trizol (Invitrogen) protocol. Two micrograms RNA from each sample was used to generate cDNA (High-Capacity cDNA Reverse Transcription Kit; Life Technologies), and QPCR was conducted using SYBR green (Invitrogen). To assess early gene expression in response to FGF21 administration, we administered vehicle or FGF21 (1 mg/kg BW) via i.p. injection to KLB AdipoKO, KLB BatKO, and WT littermates. One hour later, mice were sacrificed tissues collected, and immediately flash frozen in liquid nitrogen.

QPCR primer sequences are as follows: *Klb*: 5′-GATGAAGAATTTCCTAAACCAGGTT-3′, 5-AACCAAACACGCGGATTTC-3′; *Egr1*: 5′-CGAGCGAACAACCCTATGAG-3′, 5′-CATTATTCAGAGCGATGTCAGAAA-3′;

cFos: 5′-GGACAGCCTTTCCTACTACCATTCC-3′, 5′-AAAGTTGGCACTAGAGACGGACAGA-3′; *Bmp8b*: 5′-TCAACACAACCCTCCACATCA-3′, 5′-AGATCGGAGCGTCTGAAGATC-3′; *Zbtb16*: 5′-CCCAGTTCTCAAAGGAGGATG-3′, 5′-TTCCCACACAGCAGACAGAAG-3′; *Fgfr1ca*: 5′-TTCATCCTGGTGGTGGCAGC-3′, 5′-GCTCTTCTTGGTGCCGCTCT-3′; *U36b4*: 5′-CGTCCTCGTTGGAGTGACA-3′, 5′-CGGTGCGTCAGGGATTG-3′.

Plasma and Tissue Analysis—Human FGF21 (Biovendor), mouse insulin (Crystal Chem), mouse leptin levels (Millipore), and mouse adiponectin levels (Millipore) were measured using commercially available ELISAs. Blood was collected into 300K2E microvettes (Sarstedt) and spun at 3000 rpm for 30 minutes 4°C to separate plasma. Plasma glucose levels were measured using the glucose autokit (Wako Chemicals). Plasma triglycerides and cholesterol were measured using colorimetric assays (Infinity™, Thermo Scientific). All measurements were performed according to the manufacturer's instructions.

Hepatic triglycerides were quantified via Folch extraction. Mouse livers were collected, snap-frozen, pulverized, and stored at −80°C prior to analysis. All of the following steps were performed using glassware (not plastic). 100–200mg of snap-frozen isolated mouse liver tissue was thoroughly homogenized for 30 seconds per sample in 4 mL of a 2:1 v/v chloroform/methanol mix then allowed to equilibrate at room temperature for 30 minutes. After adding 1 ml of 50mM NaCl to each sample, the samples were vortexed for 15 seconds and centrifuged for 10 min at 1000xg at room temperature. The bottom organic phase was isolated and 1 ml of 0.36M $CaCl_2$/Methanol/H_2O mix (1:1 v/v Methanol/H_2O) was added to the samples, vortexed, and centrifuged as before. Again, the bottom organic layer was isolated and placed into 5 mL glass volumetric flasks. The flasks were then volumed up to the 5 mL mark with fresh chloroform, flasks were capped, and left overnight at room temperature. The following day, any traces of water were removed by carefully pipetting off the top aqueous layer and chloroform was replaced to the 5 mL mark as needed. 10µl of a 1:1 v/v Triton-X 100/chloroform solution was added to fresh test tubes. 10 µL of the organic solution was added to the Triton-X 100/chloroform test tubes. Blanks consisted of 10 µL of Triton-X 100/chloroform and 10 µL of pure chloroform. 10 µL of pre-determined standards (Verichem Laboratories Inc, Matrix Plus Chemistry Reference Kit, Cat. No 9500) in 10 µL of Triton-X 100/chloroform tubes were also included. Samples were allowed to air dry in a chemical hood overnight. The following day, plasma triglycerides were measured using a colorimetric assay, (InfinityTM, Thermo Scientific) following the manufacturer's instructions as follows: 1 ml of the Infinity reagent warmed to room temperature was added to each test-tube. 200µl of the blanks, standards and the samples were pipetted into a 96-well plate in duplicate and absorbance was measured on a 96-well plate reader.

Whole-body Fluorodeoxyglucose (FDG) Positron Emission Tomography (PET)/Computed Tomography (CT) Imaging—Whole-body [^{18}F]-fluorodeoxyglucose (FDG) scanning was performed in the Small Animal Imaging Core at the University of Iowa as previously reported (Morgan et al., 2015). 11–14-week old, chow-fed male WT and KLB BatKO mice were singly housed one week before the procedure and were kept singly housed throughout the fasting and uptake period. WT and KLB BatKO mice were then fasted for 5

hours and then i.p. injected with FDG (7.88 ± 0.40 MBq) and insulin (0.25 U/kg) in combination with vehicle or FGF21 (1 mg/kg). Mice were then allowed to move freely in cages with padding under a heat lamp for a 90 minute awake uptake period. Mice were then anesthetized with 1.5% isoflurane and imaged on an Inveon PET/CT/SPECT Multimodality Animal Imaging system (Siemens, Knoxville, TN). Volumes of interest were drawn manually and image analysis was completed using PMOD version 3.709 (PMOD Technologies, Zurich, Switzerland) to quantify region-specific glucose uptake. PET/CT images were generated using the multimodal 3D visualization modality in Inveon Research Workplace.

In Vivo Radioactive Glucose Uptake—In vivo radioactive glucose uptake assays were performed similarly as described (Markan et al., 2014). All mice used for in vivo radioactive glucose uptake were chow-fed 12–14 week old males with wild-type littermates used as a control. Mice were singly housed a week prior to in vivo radioactive glucose uptake. On the day of uptake assay, mice were fasted for 5 hours and were transferred to a radioactive procedure room to acclimate 1.5 hours prior to initiating the assay. FGF21 or vehicle was added to Insulin/Deoxy-D-glucose, 2-[1,2–3H (N)] (Perkin Elmer) mixture for a final dose of 1 mg/kg BW of FGF21, 0.25U Ins/kg BW, and 1.25 μCi/g BW. After injection, mice were placed back in cages and sacrificed by decapitation 90 minutes post-injection. Tissues were collected and immediately snap frozen in liquid nitrogen.

Tissues were then processed to determine levels of radioactive phosphorylated 2DG. Tissues were weighed and placed in 400μL of 1M NaOH and incubated at 85°C for 10 minutes to homogenize. Samples were then neutralized with 400μL of 1M HCl. 200μL of homogenized samples were then added to duplicate solutions of 1mL ice cold 7% perchloric acid or duplicate solutions of 1mL Somogyi buffer. Somogyi buffer was prepared immediately before use by combining 500μL 0.3N $ZnSO_4$ with 500μL 0.3N $Ba(OH)_2$. Samples were spun at 13,000×g for 5 mins at 4°C. 800 μL of supernatant was added to 10mL of Bio-Safe II Scintillation fluid (RPI) and radioactivity measured on a scintillation counter in counts per minute (c.p.m.). Phospho-2DG concentration in samples was measured by converting c.p.m. measurements to disintegrations per minute (d.p.m.) based on the scintillation counter efficiency. Average d.p.m. measured from Somogyi buffer was subtracted from average d.p.m. from perchloric acid solutions for each tissue and normalized to tissue weight.

Western Blot Analysis—For western blot analysis, snap-frozen tissues were homogenized on ice in lysis buffer containing 10 mM Tris-HCl, pH 7.4, 5 mM EDTA, 5 mM EGTA, 150 mM NaCl, 10% glycerol, 1% NP-40, 0.5% Triton X-100 and protease inhibitors. Samples were centrifuged for 5 min at 0.5 × g at 4°C and infranatant collected. An appropriate volume of 6X Laemmli buffer was added and all samples incubated at 100°C for 10 minutes and then briefly placed on ice. Protein concentration was determined by Bradford assay and then equal quantity of sample resolved by SDS-PAGE. Proteins were transferred to a PVDF membrane before being probed with the specified antibodies. Antibody information: β-actin (Sigma, #A5316), phospho-ERK1/2 (Cell Signaling, #9101), total ERK1/2 (Cell Signaling, #9102), Myc (Millipore, #05–724) and β-klotho (R&D Systems, #AF2619).

Primary White Adipocyte Isolation and Treatment—Primary white adipocytes were isolated from white fat depots of 4-day-old C57BL/6J pups (n = 14). Subcutaneous fat pads were dissected and digested (2% BSA (Sigma, FFA free) and 0.1% collagenase (Invitrogen) in HBSS (Gibco)). Digested tissue was then placed into a pre-warmed shaker (37°C) and allowed to shake at 150rpm for 1h, followed by centrifugation at 1000×g for 3min at 4°C. The supernatant was discarded and the pellet was washed and centrifuged 3 times with preadipocyte growth media (DMEM (high glucose, no pyruvate Sigma D5796), 10% fetal bovine serum (FBS; Gibco), 1X Pen-Strep (Gibco), 1X non-essential amino acids (Gibco), 1X Glutamax (Gibco), 1M HEPES (Gibco), and 0.1mM 2-mercaptoethanol (Ameresco)). After the final wash, the preadipocyte growth media was removed and the pellet was resuspended in fresh preadipocyte growth media at 2mL per pup. The resuspended cells where filtered through a 100 μm nylon filter and cells were plated in 6 well plates at 2mL per well. Finally, cells were incubated and allowed to grow for 2 days at 37°C in a cell incubator.

For differentiation, cells were reseeded into new 6-well plates containing fresh preadipocyte growth media. Briefly, media was aspirated from each well and cells were washed with room temperature 1X PBS 3 times. Next, 300μL of trypsin (Gibco) was added to each well and cells were collected and put into fresh preadipocyte growth media and seeded into new 6-well plates. Cells were allowed to grow until confluent (about 5 days; media was changed once). Cells were then differentiated using differentiation media (DMEM, 10% FBS, 1X Pen-Strep, 5μg/ml insulin (Sigma), 1μM dexamethasone (Sigma), and 0.5mM IBMX (Sigma)) for 2 days. Following differentiation into mature adipocytes, cells were put in maintenance media (DMEM, 10% FBS, 1X Pen-Strep, and 5μg/ml insulin) until used for experiment.

Mature adipocytes were treated with either vehicle or FGF21 (1μg/ml) prepared in serum free maintenance media on a time course of 0, 0.25, 0.5, 1, 2, 4, 8, 16, and 24h. Following treatments, mature adipocytes were placed on ice and media was collected from each well. Cells were washed 3 times with ice cold 1X PBS and were lysed using 250μL/well WAT lysis buffer (10mM Tris-HCL (pH 7.4; Fisher Scientific), 5mM EDTA and EGTA (Sigma), 150mM NaCl (Sigma), 10% glycerol (Sigma), 1% NP-40 (Sigma), 0.5% Triton X-100 (Sigma), and complete protease and phosphatase inhibitor cocktails (Roche)). Cell lysates were collected and put on ice. All samples were stored in a −20°C freezer until use (2 days). Adiponectin levels were measured in the media from treated cells using a commercially available ELISA (EMD Millipore).

Quantification and Statistical Analysis—Data are presented as the mean +/− SEM; $p < 0.05$ was considered significant. Student's t test was used to compare two independent groups. Two-way ANOVAs with Sidak post hoc correction (GraphPad Prism) were used for multiple group analyses.

REAGENT or RESOURCE	SOURCE	IDENTIFIER
Antibodies		

β-actin	Sigma	#A5316, RRID:AB_476743
phospho-ERK1/2	Cell Signaling	#9101, RRID:AB_331646
total ERK1/2	Cell Signaling	#9102, RRID:AB_330744
Myc	Millipore	#05–724, RRID:AB_309938
β-klotho	R&D Systems	#AF2619, AB_2131932
Chemicals, Peptides, and Recombinant Proteins		
Recombinant Human FGF21	Novo Nordisk	N/A
Human Insulin	Sigma	I9278
Critical Commercial Assays		
Human FGF21 ELISA	Biovendor	#RD191108200R
Mouse Leptin ELISA	Millipore	#EZML-82K
Mouse Insulin ELISA	Crystal Chem	#90080
Mouse Adiponectin ELISA	Millipore	#EZMADP-60K
Glucose Autokit	Wako Chemicals	#439-90901
Triglycerides reagent	Thermo Scientific	TR22421
Total Cholesterol reagent	Thermo Scientific	TR13421
Experimental Models: Cell Lines		
Primary white adipocytes	This paper	N/A
Experimental Models: Organisms/Strains		
Adiponectin KO (B6;129-*Adipoq*^{tm1Chan}/J)	The Jackson Laboratory	Stock No: 008195
KLB$^{fl/fl}$ (Klb$^{tm1.1Sakl}$)	Dr. Steven Kliewer, UTSW	N/A
Adiponectin-Cre (B6;FVB-Tg(Adipoq-cre)1Evdr/J)	The Jackson Laboratory	Stock No: 010803
Adiponectin-rtTA	Dr. Philipp Scherer, UTSW	N/A
IR$^{fl/fl}$ (B6.129S4(FVB)-*Insr* ^{tm1Khn}/J)	The Jackson Laboratory	Stock No: 006955
TRE-caFGFR1	Dr. David Ornitz, Washu	N/A
UCP1-Cre mice (B6.FVB-Tg(Ucp1-cre)1Evdr/J)	The Jackson Laboratory	Stock No: 024670
Oligonucleotides		
Primers – *Klb*: 5′-GATGAAGAATTTCCTAAACCAGGTT-3′, 5-AACCAAACACGCGGATTTC-3′	This paper	N/A

Primers – *Egr1*: 5′-CGAGCGAACAACCCTATGAG-3′, 5′-CATTATTCAGAGCGATGTCAGAAA-3′	This paper	N/A
Primers – *cFos*: 5′-GGACAGCCTTTCCTACTACCATTCC-3′, 5′-AAAGTTGGCACTAGAGACGGACAGA-3′	This paper	N/A
Primers – *Bmp8b*: 5′-TCAACACAACCCTCCACATCA-3′, 5′-AGATCGGAGCGTCTGAAGATC-3′	This paper	N/A
Primers – *Zbtb16*: 5′-CCCAGTTCTCAAAGGAGGATG-3′, 5′-TTCCCACACAGCAGACAGAAG-3′	This paper	N/A
Primers – *Fgfr1ca*: 5′-TTCATCCTGGTGGTGGCAGC-3′, 5′-GCTCTTCTTGGTGCCGCTCT-3′	This paper	N/A
Primers – *U36B4*: 5′-CGTCCTCGTTGGAGTGACA-3′, 5′-CGGTGCGTCAGGGATTG-3′	This paper	N/A
Software and Algorithms		
Graphpad Prism 7	Graphpad	http://www.graphpad.com/scientific-software/prism/
PMOD version 3.709	PMOD Technologies	http://www.pmod.com/web/
Inveon Research Workplace	Inveon	https://www.healthcare.siemens.com/molecular-imaging/preclinical-i
Other		
N/A		

Supplementary Material

Refer to Web version on PubMed Central for supplementary material.

Acknowledgments

We thank Drs. David Mangelsdorf and Steven Kliewer (Univ. of Texas Southwestern Medical Center (UTSW)) for kindly providing KLB$^{fl/fl}$ mice, and Dr. Philipp Scherer (UTSW) for generously providing Adiponectin-rtTa mice. We also thank Dr. Birgitte Andersen (Novo Nordisk) for providing FGF21 protein, and Ms. Nicole Pearson and Dr. Justin Grobe (Univ. of Iowa) for technical assistance. This work was supported by the National Institutes of Health (NIH) (R01DK106104) (M.J.P.), T32 GM067795 (L.D.B.), R01 HL111190 (D.M.O), and the University of Iowa Carver College of Medicine (M.J.P.).

References

Adams AC, Coskun T, Rovira AR, Schneider MA, Raches DW, Micanovic R, Bina HA, Dunbar JD, Kharitonenkov A. Fundamentals of FGF19 & FGF21 action in vitro and in vivo. PLoS One. 2012a; 7:e38438. [PubMed: 22675463]

Adams AC, Yang C, Coskun T, Cheng CC, Gimeno RE, Luo Y, Kharitonenkov A. The breadth of FGF21's metabolic actions are governed by FGFR1 in adipose tissue. Mol Metab. 2012b; 2:31–37. [PubMed: 24024127]

Bartelt A, Bruns OT, Reimer R, Hohenberg H, Ittrich H, Peldschus K, Kaul MG, Tromsdorf UI, Weller H, Waurisch C, et al. Brown adipose tissue activity controls triglyceride clearance. Nat Med. 2011; 17:200–205. [PubMed: 21258337]

Bruning JC, Michael MD, Winnay JN, Hayashi T, Horsch D, Accili D, Goodyear LJ, Kahn CR. A muscle-specific insulin receptor knockout exhibits features of the metabolic syndrome of NIDDM without altering glucose tolerance. Mol Cell. 1998; 2:559–569. [PubMed: 9844629]

Cannon B, Nedergaard J. Brown adipose tissue: function and physiological significance. Physiol Rev. 2004; 84:277–359. [PubMed: 14715917]

Cilvik SN, Wang JI, Lavine KJ, Uchida K, Castro A, Gierasch CM, Weinheimer CJ, House SL, Kovacs A, Nichols CG, et al. Fibroblast growth factor receptor 1 signaling in adult cardiomyocytes increases contractility and results in a hypertrophic cardiomyopathy. PLoS One. 2013; 8:e82979. [PubMed: 24349409]

Coskun T, Bina HA, Schneider MA, Dunbar JD, Hu CC, Chen Y, Moller DE, Kharitonenkov A. Fibroblast growth factor 21 corrects obesity in mice. Endocrinology. 2008; 149:6018–6027. [PubMed: 18687777]

Ding X, Boney-Montoya J, Owen BM, Bookout AL, Coate KC, Mangelsdorf DJ, Kliewer SA. betaKlotho is required for fibroblast growth factor 21 effects on growth and metabolism. Cell metabolism. 2012; 16:387–393. [PubMed: 22958921]

Eguchi J, Wang X, Yu ST, Kershaw EE, Chiu PC, Dushay J, Estall JL, Klein U, Maratos-Flier E, Rosen ED. Transcriptional Control of Adipose Lipid Handling by IRF4. Cell Metabolism. 2011; 13:249–259. [PubMed: 21356515]

Gaich G, Chien JY, Fu H, Glass LC, Deeg MA, Holland WL, Kharitonenkov A, Bumol T, Schilske HK, Moller DE. The effects of LY2405319, an FGF21 analog, in obese human subjects with type 2 diabetes. Cell Metab. 2013; 18:333–340. [PubMed: 24011069]

Harno E, Cottrell EC, White A. Metabolic pitfalls of CNS Cre-based technology. Cell Metab. 2013; 18:21–28. [PubMed: 23823475]

Holland WL, Adams AC, Brozinick JT, Bui HH, Miyauchi Y, Kusminski CM, Bauer SM, Wade M, Singhal E, Cheng CC, et al. An FGF21-adiponectin-ceramide axis controls energy expenditure and insulin action in mice. Cell Metab. 2013; 17:790–797. [PubMed: 23663742]

Kurosu H, Choi M, Ogawa Y, Dickson AS, Goetz R, Eliseenkova AV, Mohammadi M, Rosenblatt KP, Kliewer SA, Kuro-o M. Tissue-specific expression of betaKlotho and fibroblast growth factor (FGF) receptor isoforms determines metabolic activity of FGF19 and FGF21. J Biol Chem. 2007; 282:26687–26695. [PubMed: 17623664]

Lin Z, Tian H, Lam KS, Lin S, Hoo RC, Konishi M, Itoh N, Wang Y, Bornstein SR, Xu A, et al. Adiponectin mediates the metabolic effects of FGF21 on glucose homeostasis and insulin sensitivity in mice. Cell Metab. 2013; 17:779–789. [PubMed: 23663741]

Ma K, Cabrero A, Saha PK, Kojima H, Li L, Chang BH, Paul A, Chan L. Increased beta -oxidation but no insulin resistance or glucose intolerance in mice lacking adiponectin. J Biol Chem. 2002; 277:34658–34661. [PubMed: 12151381]

Markan KR, Naber MC, Ameka MK, Anderegg MD, Mangelsdorf DJ, Kliewer SA, Mohammadi M, Potthoff MJ. Circulating FGF21 is liver derived and enhances glucose uptake during refeeding and overfeeding. Diabetes. 2014; 63:4057–4063. [PubMed: 25008183]

Markan KR, Potthoff MJ. Metabolic fibroblast growth factors (FGFs): Mediators of energy homeostasis. Semin Cell Dev Biol. 2015

Morgan DA, McDaniel LN, Yin T, Khan M, Jiang J, Acevedo MR, Walsh SA, Ponto LL, Norris AW, Lutter M, et al. Regulation of glucose tolerance and sympathetic activity by MC4R signaling in the lateral hypothalamus. Diabetes. 2015; 64:1976–1987. [PubMed: 25605803]

Muise ES, Souza S, Chi A, Tan Y, Zhao X, Liu F, Dallas-Yang Q, Wu M, Sarr T, Zhu L, et al. Downstream signaling pathways in mouse adipose tissues following acute in vivo administration of fibroblast growth factor 21. PLoS One. 2013; 8:e73011. [PubMed: 24039848]

Ogawa Y, Kurosu H, Yamamoto M, Nandi A, Rosenblatt KP, Goetz R, Eliseenkova AV, Mohammadi M, Kuro-o M. BetaKlotho is required for metabolic activity of fibroblast growth factor 21. Proceedings of the National Academy of Sciences of the United States of America. 2007; 104:7432–7437. [PubMed: 17452648]

Orava J, Nuutila P, Lidell ME, Oikonen V, Noponen T, Viljanen T, Scheinin M, Taittonen M, Niemi T, Enerback S, et al. Different metabolic responses of human brown adipose tissue to activation by cold and insulin. Cell Metab. 2011; 14:272–279. [PubMed: 21803297]

Owen BM, Ding X, Morgan DA, Coate KC, Bookout AL, Rahmouni K, Kliewer SA, Mangelsdorf DJ. FGF21 acts centrally to induce sympathetic nerve activity, energy expenditure, and weight loss. Cell Metab. 2014; 20:670–677. [PubMed: 25130400]

Rosen ED, Spiegelman BM. What we talk about when we talk about fat. Cell. 2014; 156:20–44. [PubMed: 24439368]

Schlein C, Talukdar S, Heine M, Fischer AW, Krott LM, Nilsson SK, Brenner MB, Heeren J, Scheja L. FGF21 Lowers Plasma Triglycerides by Accelerating Lipoprotein Catabolism in White and Brown Adipose Tissues. Cell Metab. 2016; 23:441–453. [PubMed: 26853749]

Sun K, Wernstedt Asterholm I, Kusminski CM, Bueno AC, Wang ZV, Pollard JW, Brekken RA, Scherer PE. Dichotomous effects of VEGF-A on adipose tissue dysfunction. Proc Natl Acad Sci U S A. 2012; 109:5874–5879. [PubMed: 22451920]

Talukdar S, Zhou Y, Li D, Rossulek M, Dong J, Somayaji V, Weng Y, Clark R, Lanba A, Owen BM, et al. A Long-Acting FGF21 Molecule, PF-05231023, Decreases Body Weight and Improves Lipid Profile in Non-human Primates and Type 2 Diabetic Subjects. Cell Metab. 2016; 23:427–440. [PubMed: 26959184]

Veniant MM, Hale C, Helmering J, Chen MM, Stanislaus S, Busby J, Vonderfecht S, Xu J, Lloyd DJ. FGF21 promotes metabolic homeostasis via white adipose and leptin in mice. PLoS One. 2012; 7:e40164. [PubMed: 22792234]

von Holstein-Rathlou S, BonDurant LD, Peltekian L, Naber MC, Yin TC, Claflin KE, Urizar AI, Madsen AN, Ratner C, Holst B, et al. FGF21 Mediates Endocrine Control of Simple Sugar Intake and Sweet Taste Preference by the Liver. Cell Metab. 2016; 23:335–343. [PubMed: 26724858]

Wu AL, Kolumam G, Stawicki S, Chen Y, Li J, Zavala-Solorio J, Phamluong K, Feng B, Li L, Marsters S, et al. Amelioration of type 2 diabetes by antibody-mediated activation of fibroblast growth factor receptor 1. Sci Transl Med. 2011; 3:113ra126.

Xu J, Lloyd DJ, Hale C, Stanislaus S, Chen M, Sivits G, Vonderfecht S, Hecht R, Li YS, Lindberg RA, et al. Fibroblast growth factor 21 reverses hepatic steatosis, increases energy expenditure, and improves insulin sensitivity in diet-induced obese mice. Diabetes. 2009a; 58:250–259. [PubMed: 18840786]

Xu J, Stanislaus S, Chinookoswong N, Lau YY, Hager T, Patel J, Ge H, Weiszmann J, Lu SC, Graham M, et al. Acute glucose-lowering and insulin-sensitizing action of FGF21 in insulin-resistant mouse models–association with liver and adipose tissue effects. Am J Physiol Endocrinol Metab. 2009b; 297:E1105–1114. [PubMed: 19706786]

Highlights

- FGF21 signaling to adipose tissues is required for acute insulin sensitization
- Adiponectin is dispensable for the metabolic effects of FGF21
- FGF21 reduces body weight by signaling to non-adipose tissues
- FGF21 signals to brown adipocytes to mediate its acute glucose-lowering effects

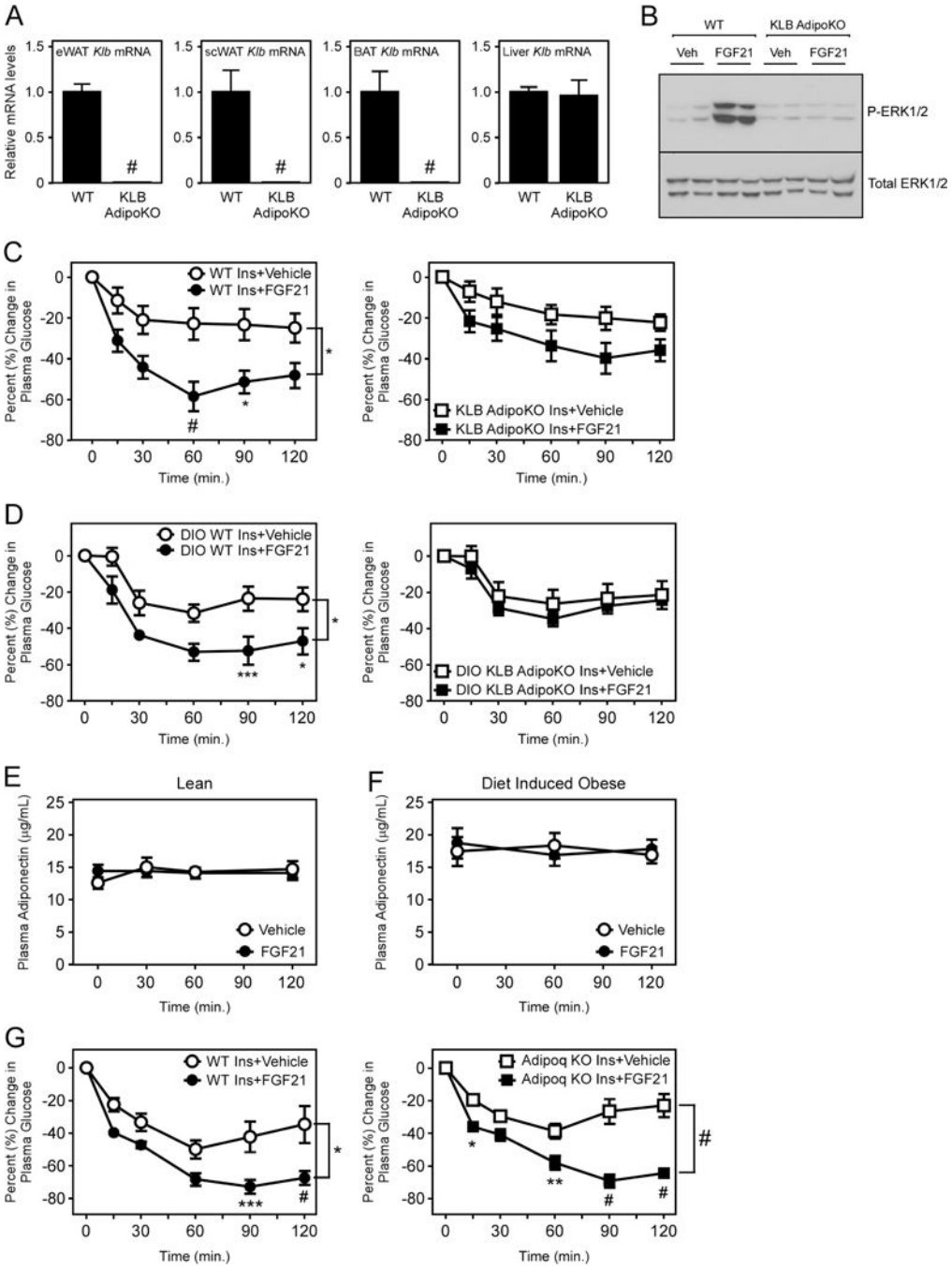

Figure 1. FGF21 signaling to adipose tissues is required for its acute, insulin-sensitizing effects but does not require adiponectin

(A) *Klb* mRNA levels in epididymal WAT (eWAT), subcutaneous WAT (scWAT), interscapular BAT, and liver of 12–13 week old wild-type (WT) and β-klotho adipose-specific knockout mice (KLB AdipoKO) (n = 6/group). (B) Western blot analysis of phospho-ERK1/2 and total ERK1/2 levels from eWAT of 12–13 week old WT and KLB AdipoKO mice administered vehicle (Veh) or FGF21 (1 mg/kg) for 15 minutes. (C) Percent change in plasma glucose levels in lean, 12–14 week old, male KLB AdipoKO mice and WT littermate controls co-injected with insulin and either vehicle or FGF21 (1 mg/kg) (n = 6/

group). (D) Percent change in plasma glucose levels in 16–18 week old male, diet-induced obese (DIO) KLB AdipoKO mice and WT littermate controls on co-injected with insulin and either vehicle or FGF21 (1 mg/kg) (n = 5-6/group). Plasma adiponectin levels at the indicated time points in (E) 12–13 week old, chow-fed male WT (KLBfl/fl) and (F) DIO 16–18 week old male WT (KLBfl/fl) mice on high fat diet for 12 weeks after i.p. administration of vehicle or FGF21 (1 mg/kg) (n = 8/group). (G) Percent change in plasma glucose levels in 12–14 week old, male WT (+/+ and +/−) and Adiponectin knockout (Adipoq KO) littermates co-injected with insulin and either vehicle or FGF21 (1 mg/kg) (n = 6/group). Values are mean +/− SEM. (*, $P< 0.05$; **, $P<0.01$; ***, $P< 0.005$; and #, $P<0.001$).

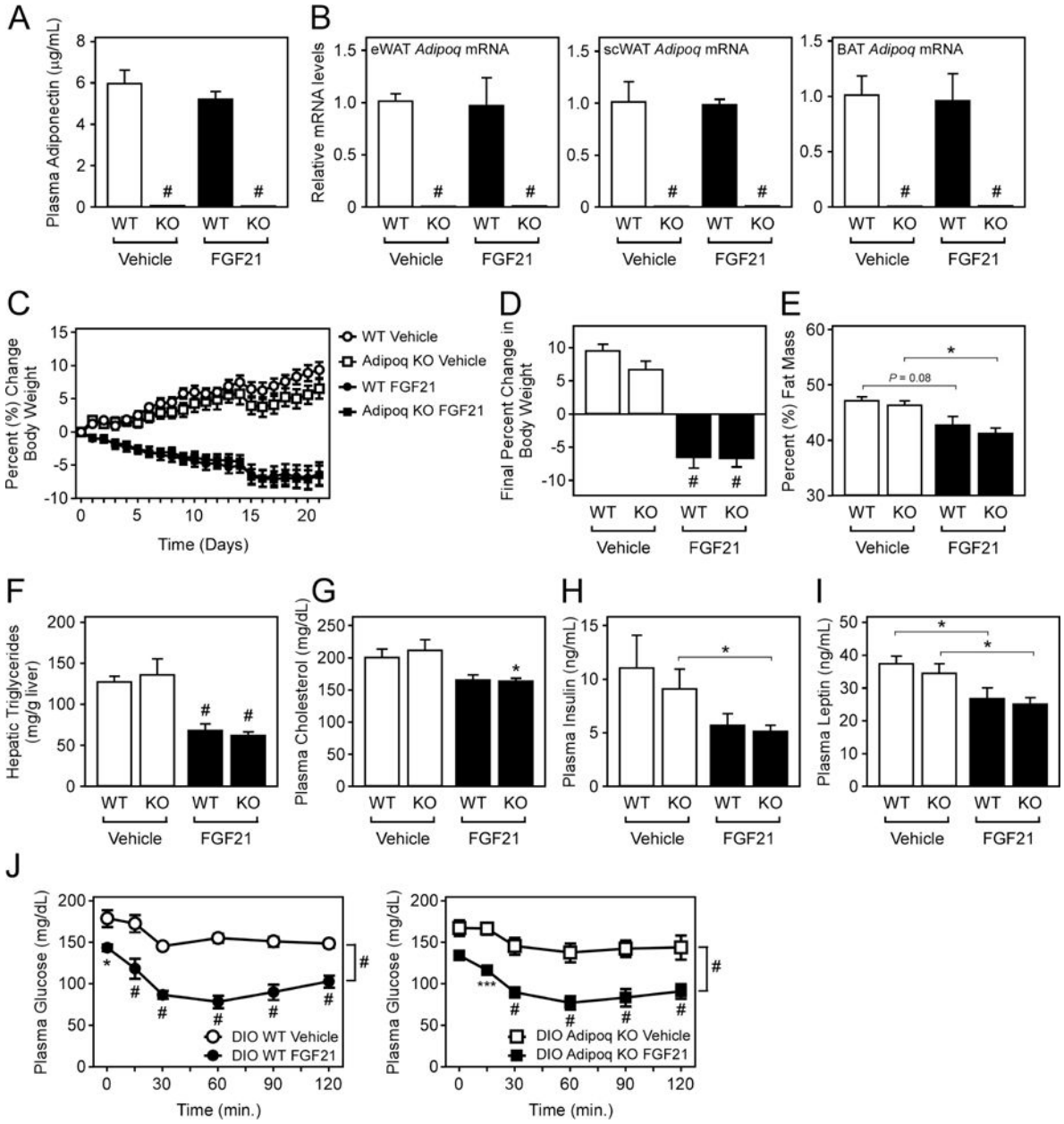

Figure 2. Adiponectin is dispensable for the chronic effects of FGF21 on energy expenditure and insulin sensitivity

(A–J) 16–18 week old DIO WT and Adipoq KO mice were administered vehicle or FGF21 (1 mg/kg) via i.p. injection daily for 3 weeks (n = 5–9/group). (A) Plasma adiponectin levels, (B) *Adipoq* mRNA levels in the indicated tissues, (C) daily percent change in body weight, (D) final percent change in body weight, (E) percent fat mass, (F) hepatic triglyceride levels, (G) plasma cholesterol, (H) plasma insulin and (I) plasma leptin levels in DIO WT and Adipoq KO mice administered vehicle or FGF21 for 3 weeks. (J) Insulin tolerance tests in DIO WT and Adipoq KO mice after 3 weeks (n = 5–7/group). Values are mean +/− SEM. (*, $P< 0.05$; **, $P<0.01$; ***, $P< 0.005$; and #, P<0.001).

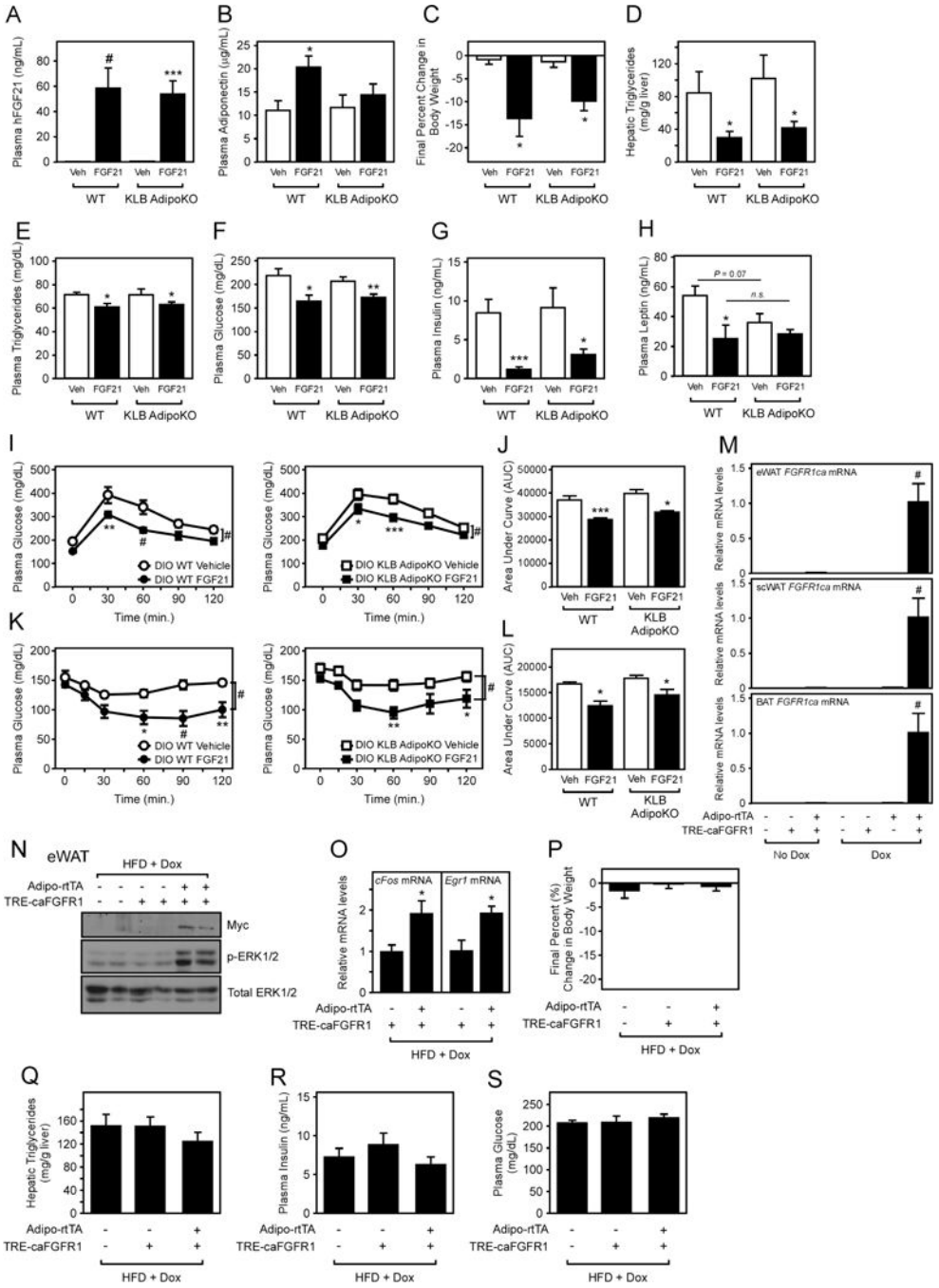

Figure 3. The energy expending effects of FGF21 do not require direct signaling to adipose tissue

(A–H) 16–18 week old DIO WT and KLB AdipoKO were implanted with osmotic minipumps delivering vehicle or FGF21 (1 mg/kg/day) for 2 weeks. (A) Plasma human FGF21, (B) plasma adiponectin, (C) final percent change in body weight, (D) hepatic triglycerides, (E) plasma triglycerides, (F) plasma glucose, (G) plasma insulin, and (H) plasma leptin levels in the indicated mice (n = 5–7/group). (I) Glucose tolerance tests in DIO WT and KLB AdipoKO mice after 2 weeks daily i.p. injection of vehicle or FGF21 (1 mg/kg) (n = 5–8/group). (J) Area under the curve (AUC) for mice in (I). (K) Insulin

tolerance tests in DIO WT and KLB AdipoKO mice after 3 weeks daily i.p. injection of vehicle or FGF21 (1 mg/kg) (n = 5–8/group). (L) Area under the curve for mice in (K). (M) ca*FGFR1* mRNA levels in eWAT, scWAT, and BAT of WT, Adipo-rtTA transgenic, TRE-caFGFR1 transgenic, and Adipo-rtTA/TRE-caFGFR1 double transgenic mice provided water with or without doxycycline (DOX) for 5 days. (N–S) WT, TRE-caFGFR1 transgenic, and Adipo-rtTA/TRE-caFGFR1 double transgenic mice were induced to obesity by 12 weeks of HFD feeding. Groups of mice were then switched to HFD + DOX for 2 weeks (n = 7–10/group). (N) Western blot analysis of Myc and phospho-ERK1/2 levels in eWAT from mice with the indicated genotypes. (O) *Egr1* and *cFos* mRNA expression in eWAT of the indicated mice. (P) Final percent body weight change, (Q) hepatic triglycerides, (R) plasma insulin, and (S) plasma glucose levels in the indicated mice on HFD + DOX for 2 weeks. Values are mean +/− SEM. (*, $P< 0.05$; **, $P<0.01$; ***, $P< 0.005$; and #, $P<0.001$).

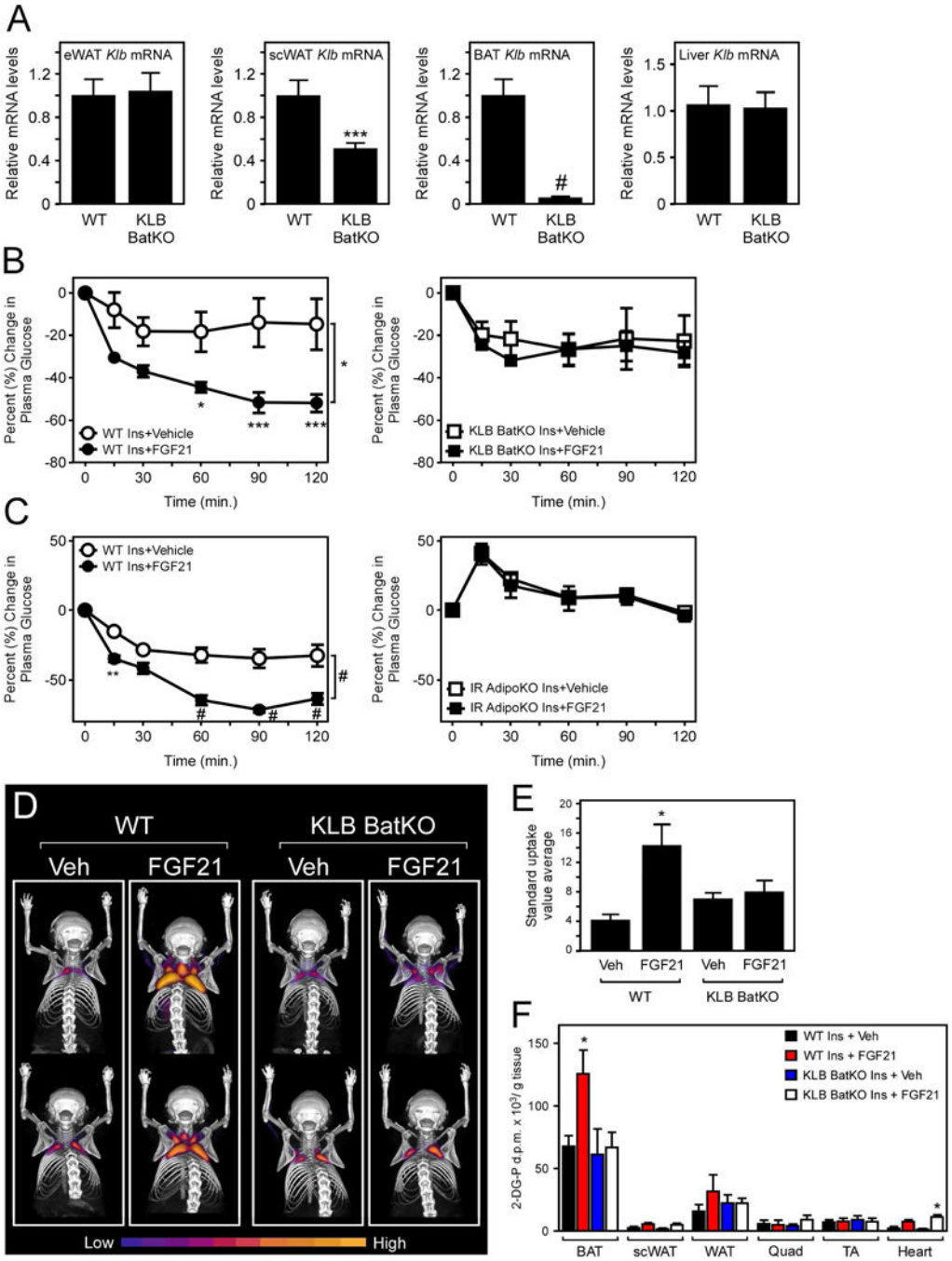

Figure 4. FGF21 signaling to brown adipocytes is required for its acute, insulin-sensitizing effects

(A) *Klb* mRNA levels in eWAT, scWAT, BAT, and liver of 12–14 week old WT and β-klotho brown adipose-specific knockout mice (KLB BatKO) (n = 6/group). (B) Percent change in plasma glucose levels in 12–14 week old, male KLB BatKO mice and WT controls co-injected with insulin and either vehicle or FGF21 (1 mg/kg) (n = 6/group). (C) Percent change in plasma glucose levels in 12–14 week old, male adipose-specific insulin receptor knockout (IR AdipoKO) mice and WT controls co-injected with insulin and either vehicle or FGF21 (1 mg/kg) (n = 5–7/group). (D) PET/CT images of relative [^{18}F]-FDG uptake in WT

and KLB BatKO mice co-injected with insulin and either vehicle or FGF21 (1 mg/kg). (E) Average standard uptake value in interscapular BAT of the indicated mice (n = 5–8/group). (F) Tissue-specific glucose uptake assays using [^{3}H]-2-deoxyglucose in WT and KLB BatKO mice co-injected with insulin and either vehicle or FGF21 (1 mg/kg) for 90 minutes (n = 5–13/group). Values are mean +/− SEM. (*, $P< 0.05$; **, $P<0.01$; ***, $P< 0.005$; and #, $P<0.001$).